Nanostructures

DOI: 10.1002/anie.200700197

Superparamagnetic Magnetite Colloidal Nanocrystal Clusters**

*Jianping Ge, Yongxing Hu, Maurizio Biasini, Ward P. Beyermann, and Yadong Yin**

Recent advances in colloidal synthesis have enabled the preparation of high-quality nanocrystals with controlled size and shape.[1–5] The focus of synthetic efforts appears to be shifting to creation of secondary structures of nanocrystals, either by self-assembly or through direct solution growth. This trend is evidenced by a number of interesting works published in the past two years.[6–10] Manipulation of the secondary structures of nanocrystals is desired in order to combine the ability to harness the size-dependent properties of individual nanocrystals with the possibility to tune collective properties due to interactions between the subunits. Herein we report the synthesis of highly water dispersible magnetite (Fe_3O_4) colloidal nanocrystal clusters (CNCs) with uniform size from about 30 to about 180 nm, each of which is composed of many single magnetite crystallites approximately 10 nm in size. The CNCs show superparamagnetic properties at room temperature, whereas a single-crystalline magnetite particle within the same size range would exhibit ferromagnetic behavior. Apparently, the magnetic interactions among crystallites within a CNC are perturbed sufficiently from the case of a single-crystalline particle that the superparamagnetic–ferromagnetic transition is suppressed. The superparamagnetic behavior, high magnetization, and high water dispersibility make these CNCs ideal candidates for various important applications such as drug delivery, bioseparation, and magnetic resonance imaging.

Superparamagnetic nanocrystals have proved to be very promising for biomedical applications, as they are not subject to strong magnetic interactions in dispersion.[11,12] Iron oxide nanocrystals have received the most attention for this purpose because of their biocompatibility and stability under physiological conditions. Several robust approaches have been developed for synthesizing magnetic iron oxide (e.g., γ-Fe_2O_3 or Fe_3O_4) nanocrystals with tightly controlled size distribution, typically by organometallic processes at elevated temperatures in nonpolar solvents.[13–16] Additional steps of surface modification or lipid encapsulation are usually performed to transfer the hydrophobic nanocrystals from nonpolar solvent to water for biomedical applications.[17,18] The nanocrystals prepared by these methods, with dimensions on the order of 10 nm, have a low magnetization per particle, so that it is difficult to effectively separate them from solution or control their movement in blood by using moderate magnetic fields. This limits their usage in some practical applications such as separation and targeted delivery. Increasing the nanocrystal size increases the saturation magnetization, but also induces the superparamagnetic–ferromagnetic transition (at a domain size of ca. 30 nm for Fe_3O_4), so that nanocrystals are no longer dispersible in solution. The strategy of forming clusters of magnetite nanocrystals has the advantage of increasing the magnetization in a controllable manner while retaining the superparamagnetic characteristics.

Highly water dispersible magnetite CNCs were synthesized by using a high-temperature hydrolysis reaction with poly(acrylic acid), PAA, as surfactant. Iron(III) chloride was used as precursor, and diethylene glycol (DEG, a polyhydric alcohol with a boiling point of 244–245 °C) as polar solvent. Poly(acrylic acid) was selected because of the strong coordination of carboxylate groups with iron cations on the magnetite surface. An additional advantage of PAA is that extension of the uncoordinated carboxylate groups on the polymer chains into aqueous solution confers on the particles a high degree of dispersibility in water. Introduction of NaOH into the hot mixture of DEG, $FeCl_3$, and PAA produces water molecules and also increases the alkalinity of the reaction system, and both results favor the hydrolysis of $FeCl_3$. Under the reductive atmosphere provided by DEG at high temperature,[3,19] $Fe(OH)_3$ partially transforms into $Fe(OH)_2$, and finally Fe_3O_4 particles are formed through dehydration. Under optimized conditions, these Fe_3O_4 nanocrystals spontaneously aggregate to form flowerlike three-dimensional clusters, as shown in the representative transmission electron microscopy (TEM) images in Figure 1. Close inspection of these images confirms that these monodisperse colloids consist of small primary particles.

The size of the CNCs can be precisely controlled from about 30 to about 180 nm by simply increasing the amount of NaOH while keeping all other parameters fixed (Figure 1). This size tunability may be the result of slight differences in H_2O concentration and alkalinity caused by varying additions of NaOH. Higher H_2O concentration and stronger alkalinity could accelerate the hydrolysis of $FeCl_3$ and promote the formation of larger oxide clusters. The growth of CNCs follows the well-documented two-stage growth model in which primary nanocrystals nucleate first in a supersaturated solution and then aggregate into larger secondary particles.[20]

[*] Dr. J. Ge, Y. Hu, Prof. Y. Yin
Department of Chemistry
University of California, Riverside, CA 92521 (USA)
Fax: (+1) 951-827-4713
E-mail: yadong.yin@ucr.edu
Dr. M. Biasini, Prof. W. P. Beyermann
Department of Physics and Astronomy
University of California, Riverside, CA 92521 (USA)

[**] Y.Y. thanks the University of California, Riverside for startup funds. We thank Dr. J. Guo and Dr. C. Dong at the Lawrence Berkeley National Laboratory for help with the XAS analyses, and Dr. K. N. Bozhilov and Mr. S. McDaniel at the Central Facility for Advanced Microscopy and Microanalysis at UCR for assistance with the TEM measurements.

Supporting information for this article is available on the WWW under http://www.angewandte.org or from the author.

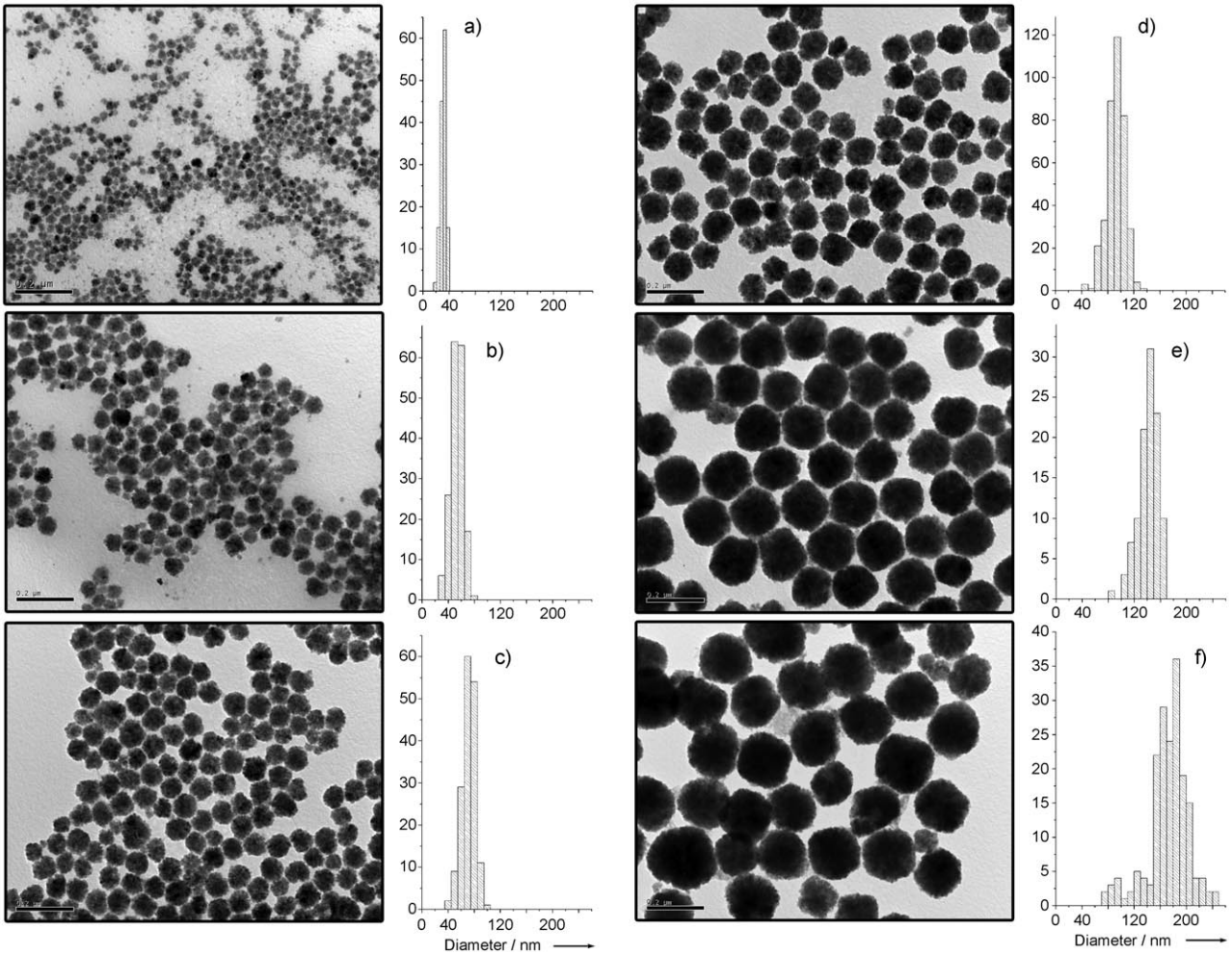

Figure 1. Representative TEM images of magnetite CNCs at the same magnification. The average diameters of the CNCs, obtained by measuring about 150 clusters for each sample, are 31 (a), 53 (b), 71 (c), 93 (d), 141 (e), and 174 nm (f). All scale bars are 200 nm.

The secondary structure of CNCs can be observed more clearly in Figure 2 for isolated clusters approximately 31, 93, and 174 nm in size. Lattice fringes were recorded for a small cluster with diameter of 31 nm, as shown in the high-resolution TEM (HRTEM) image in Figure 2a. Clearly, the cluster is composed of small primary crystals with a size of 6–8 nm and the same crystal orientation. Measuring the distance between two adjacent planes in a specific direction gives a value of 0.482 nm, which corresponds to the lattice spacing of (111) planes of cubic magnetite. The fact that primary particles crystallographically align with adjacent ones can be understood as the result of oriented attachment and subsequent high-temperature sintering during synthesis.[6] Figure 2b,c shows the secondary structures of CNCs of much larger size. The selected-area electron diffraction (SAED) pattern recorded on an isolated cluster about 174 nm in size reveals single-crystal-like diffraction (Figure 2d). The diffraction spots are widened into narrow arcs that indicate slight misalignments among the primary nanocrystals.

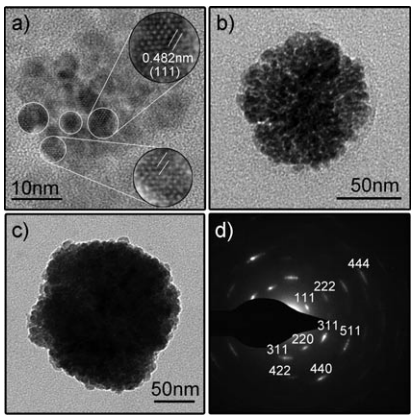

Figure 2. a) Typical HRTEM image of a 31-nm cluster. b, c) High-magnification TEM images of 93- and 174-nm CNCs. d) SAED pattern of the cluster in (c).

X-ray diffraction measurements also confirm the secondary structure of magnetite CNCs. Figure 3 shows diffraction patterns with almost identical broadenings for clusters of different sizes. Calculations with the Debye–Scherrer formula for the strongest peak (311) gave grain sizes of 9.73, 9.65, and 10.83 nm for CNCs with sizes of 53, 93, and 174 nm, respectively; this implies that the primary nanocrystals do not grow significantly with increasing size of CNCs. Consistently, the peak shape and broadening in XRD patterns of

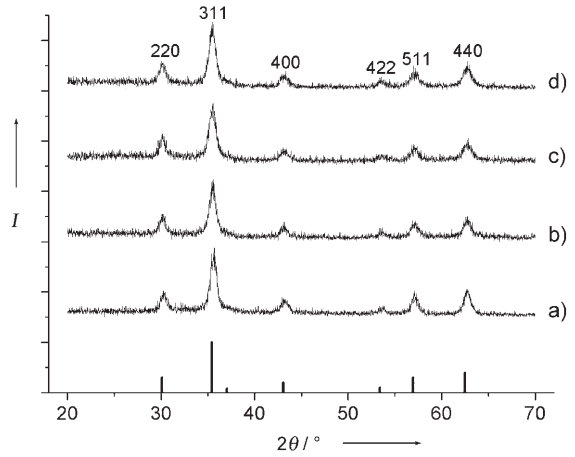

Figure 3. X-ray powder diffraction patterns of 8-nm magnetite nanodots (a) and 53- (b), 93- (c), and 174-nm magnetite CNCs (d). Literature values for the peak positions and intensities for bulk magnetite samples are indicated by the vertical bars.

CNCs are comparable to that of 8-nm isolated nanodots. We also confirmed the composition of iron oxide as magnetite by combining the XRD results with the X-ray absorption spectroscopy (XAS) measurements (see the Supporting Information).

The unique and complex structure allows CNCs to retain superparamagnetic behavior at room temperature even though their size exceeds 30 nm. Figure 4 a, b shows hysteresis loops of 93-nm CNCs measured at 300 and 2 K, respectively. The clusters show no remanence or coercivity at 300 K, that is, superparamagnetic behavior. At 2 K, thermal energy is insufficient to induce moment randomization, so that the clusters show typical ferromagnetic hysteresis loops with a remanence of 12.6 emu g^{-1} and a coercivity of 140 Oe.

To evaluate the magnetic response of CNCs to an external field, the mass magnetization σ was measured at 300 K by cycling the field between −20 and 20 kOe. Figure 4 c shows that all the CNCs, as well as the reference sample of 8-nm Fe_3O_4 nanodots, are superparamagnetic at room temperature. The saturation magnetization σ_s of PAA-covered particles was determined to be 63.5, 56.7, 30.9, and 21.2 emu g^{-1} for 174-, 93-, 53-nm CNCs, and 8-nm particles respectively. The values for the larger clusters are close, but they decrease noticeably for small particles, which may be attributed to the higher weight fraction of PAA in small particles or a surface-related effect such as surface disorder. The magnetic moment μ of an individual grain can be determined by the Langevin paramagnetic function: $M(x) = N\mu[\coth x - (1/x)]$, where $x = \mu H/k_B T$, N is the number of clusters, H the applied field, k_B the Boltzmann constant, and T the absolute temperature. Fitting the data in Figure 4 c to this function, we found magnetic moments for an 8-nm dot and 53-, 93-, and 174-nm single clusters of 8.45×10^{-17}, 3.23×10^{-14}, 1.79×10^{-13}, and 7.13×10^{-13} emu, respectively (see the Supporting Information). The dramatic increase in μ with increasing size (inset of Figure 4 c) indicates that a single CNC would have much stronger response to external field than a single nanodot.

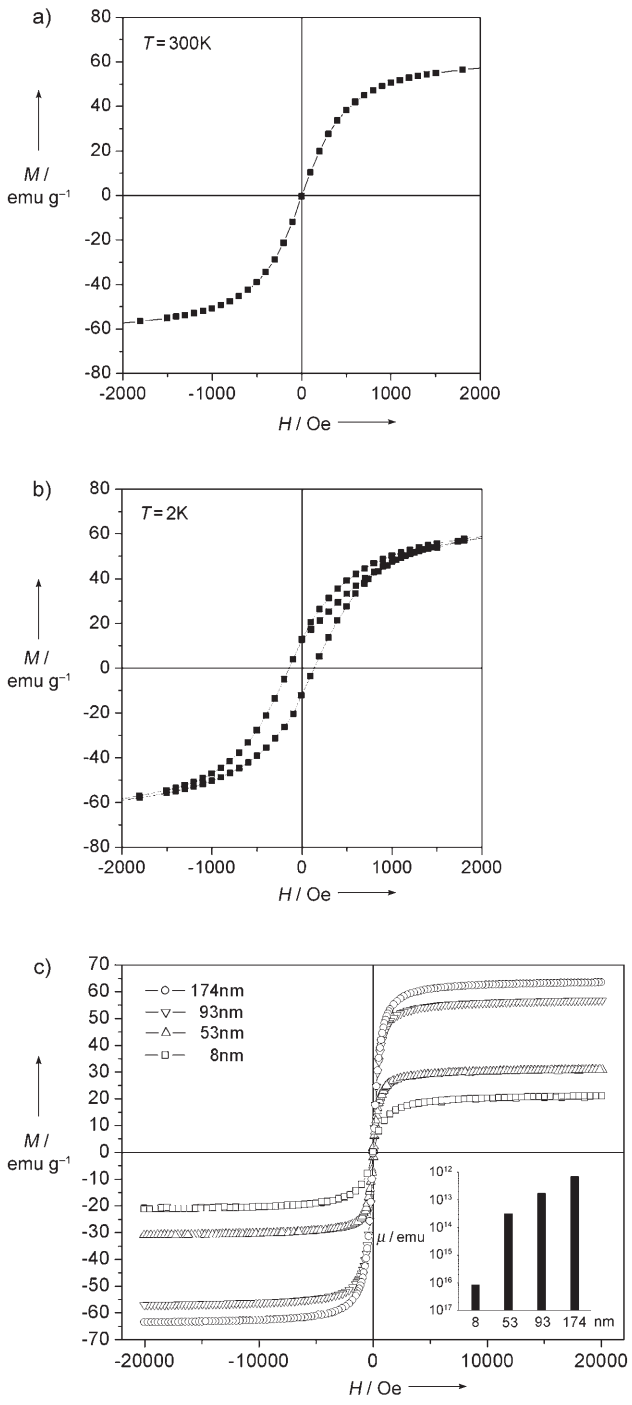

Figure 4. Mass magnetization M as a function of applied external field H measured for 93-nm CNCs at a) 300 and b) 2 K. c) Comparison of hysteresis loops of 53-, 93-, and 174-nm CNCs and a reference sample of 8-nm nanodots. Inset: Magnetic moment μ per cluster (or dot) in a logarithmic plot.

The CNCs are highly water dispersible, even after washing three times with ethanol/water, thanks to the robust surface coating of PAA. We were able to visualize the magnetic responses in an optical microscope by observing a thin layer of an aqueous dispersion of CNCs on a glass substrate. As shown in Figure 5 a–c, the initially well-dispersed CNCs formed chainlike structures when a magnetic field was

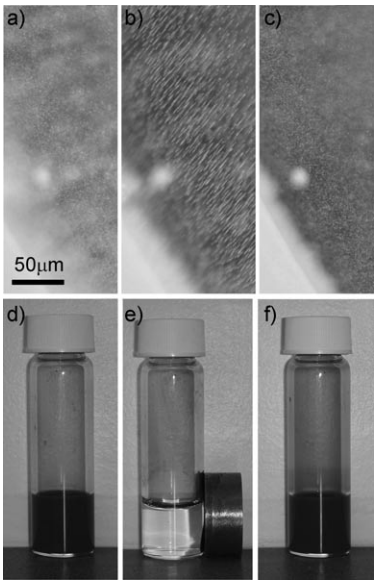

Figure 5. Superparamagnetic behavior of magnetite CNCs. Optical dark-field images of a thin layer of CNC aqueous dispersion on a glass substrate a) without magnetic field, b) with magnetic field, and c) after the applied magnetic field is removed. The bright region at the lower-left corner in each image represents the dried CNCs. Photographs of an aqueous CNC dispersion in a vial d) without magnetic field, e) with magnetic field for 1 min, and f) after the applied magnetic field is removed.

applied. The chainlike structures disassembled immediately on removing the external field, which is a typical superparamagnetic behavior. If a CNC solution is subjected to a strong magnetic field, the particles can be completely separated from the solution within minutes, as shown in Figure 5 d, e. Slight agitation will bring the CNCs back into the original solution if the magnetic field is removed (Figure 5 f).

In summary, a high-temperature solution-phase process has been developed to synthesize monodisperse magnetite colloidal clusters which are composed of small primary nanocrystals. The cluster size can be tuned precisely from about 30 to about 180 nm by simply changing the rate of hydrolysis with NaOH. Surface-tethered PAA chains render the clusters highly water-dispersible. The CNCs show superparamagnetic behavior at room temperature, and their response to external magnetic field is much stronger than that of individual magnetite nanodots due to much higher magnetization per particle. These properties are very important, especially in biomedical applications where strong magnetic response is usually achieved by embedding many magnetic nanodots in polymer beads. The sizes of these polymer beads are typically on the order of micrometers, as it is difficult to achieve a dense loading of small magnetic particles. For applications such as targeted drug delivery, embedding CNCs, instead of a collection of smaller separated superparamagnetic nanodots, within a carrier particle should enable great reduction of the overall size of the carrier. This is highly advantageous, as narrower blood capillaries may be accessed without clogging while still retaining the combination of a strong magnetic response and superparamagnetism. We also expect that facile coating of CNCs with a layer of silica will allow utilization of well-developed silane chemistry for linking specific ligands to the surface of these magnetic clusters through various coupling agents.[21]

Experimental Section

The CNCs were synthesized in solution phase at high temperature. An NaOH/DEG stock solution was prepared by dissolving NaOH (50 mmol) in DEG (20 mL); this solution was heated at 120 °C for 1 h under nitrogen, cooled, and kept at 70 °C. In a typical synthesis, a mixture of PAA (4 mmol), $FeCl_3$ (0.4 mmol), and DEG (17 mL) was heated to 220 °C in a nitrogen atmosphere for 30 min with vigorous stirring to form a transparent, light yellow solution. NaOH/DEG stock solution (1.75 mL) was injected rapidly into the above hot mixture, and the temperature dropped to about 210 °C instantly. The reaction solution slowly turned black after about 2 min and became slightly turbid. The resulting mixture was further heated for 1 h to yield 93-nm magnetite clusters. The amount of NaOH/DEG solution determines the size of the CNCs. For example, amounts of stock solution of 1.6, 1.65, 1.7, 1.8, 1.85 mL lead to CNCs with average sizes of 31, 53, 71, 141, and 174 nm, respectively. The final products were washed with a mixture of deionized water and ethanol several times and then dispersed in deionized water.

Received: January 16, 2007
Published online: April 30, 2007

Keywords: colloids · crystal growth · magnetic properties · nanostructures · oxides

[1] Y. Yin, A. P. Alivisatos, *Nature* **2005**, *437*, 664.
[2] Z. A. Peng, X. Peng, *J. Am. Chem. Soc.* **2002**, *124*, 3343.
[3] Y. Sun, Y. Xia, *Science* **2002**, *298*, 2176.
[4] X. Wang, J. Zhuang, Q. Peng, Y. D. Li, *Nature* **2005**, *437*, 121.
[5] M. P. Pileni, *Nat. Mater.* **2003**, *2*, 145.
[6] A. Narayanaswamy, H. Xu, N. Pradhan, X. Peng, *Angew. Chem.* **2006**, *118*, 5487; *Angew. Chem. Int. Ed.* **2006**, *45*, 5361.
[7] E. V. Shevchenko, D. V. Talapin, N. A. Kotov, S. O'Brien, C. B. Murray, *Nature* **2006**, *439*, 55.
[8] L. M. Dillenback, G. P. Goodrich, C. D. Keating, *Nano Lett.* **2006**, *6*, 16.
[9] J. Lee, A. O. Govorov, N. A. Kotov, *Angew. Chem.* **2005**, *117*, 7605; *Angew. Chem. Int. Ed.* **2005**, *44*, 7439.
[10] J. E. Halpert, V. J. Porter, J. P. Zimmer, M. G. Bawendi, *J. Am. Chem. Soc.* **2006**, *128*, 12590.
[11] H. Gu, K. Xu, C. Xu, B. Xu, *Chem. Commun.* **2006**, 941.
[12] Y. W. Jun, Y. M. Huh, J. S. Choi, J. H. Lee, H. T. Song, S. J. Kim, S. Yoon, K. S. Kim, J. S. Shin, J. S. Suh, J. Cheon, *J. Am. Chem. Soc.* **2005**, *127*, 5732.
[13] T. Hyeon, S. S. Lee, J. Park, Y. Chung, H. B. Na, *J. Am. Chem. Soc.* **2001**, *123*, 12798.
[14] S. Sun, H. Zeng, *J. Am. Chem. Soc.* **2002**, *124*, 8204.
[15] M. F. Casula, Y. W. Jun, D. J. Zaziski, E. M. Chan, A. Corrias, A. P. Alivisatos, *J. Am. Chem. Soc.* **2006**, *128*, 1675.
[16] A. L. Willis, N. J. Turro, S. O'Brien, *Chem. Mater.* **2005**, *17*, 5970.
[17] W. W. Yu, E. Chang, C. M. Sayes, R. Drezek, V. L. Colvin, *Int. J. Nanotechnol.* **2006**, *17*, 4483.
[18] J. Xie, S. Peng, N. Brower, N. Pourmand, S. X. Wang, S. Sun, *Pure Appl. Chem.* **2006**, *78*, 1003.
[19] H. Deng, X. L. Li, Q. Peng, X. Wang, J. P. Chen, Y. D. Li, *Angew. Chem.* **2005**, *117*, 2842; *Angew. Chem. Int. Ed.* **2005**, *44*, 2782.
[20] S. Libert, V. Gorshkov, D. Goia, E. Matijeviæ, V. Privman, *Langmuir* **2003**, *19*, 10679.
[21] Y. Lu, Y. Yin, B. T. Mayers, Y. Xia, *Nano Lett.* **2002**, *2*, 183.

